Acta Neurochir (2002) [Suppl] 81: 59–63

Communicating Hydrocephalus: The Biomechanics of Progressive Ventricular Enlargement Revisited

A. Peña[1,2,4], N. G. Harris[1,2,3], M. D. Bolton[4], M. Czosnyka[1,2,3], and J. D. Pickard[1,2,3]

[1] Academic Neurosurgery Unit, University of Cambridge, UK
[2] Wolfson Brain Imaging Centre, University of Cambridge, UK
[3] Cambridge Centre for Brain Repair, University of Cambridge, UK
[4] Department of Engineering, University of Cambridge, UK

Summary

Background. This article investigates the physical mechanisms involved in the chronic ventricular enlargement that accompanies communicating hydrocephalus (CH) – including its normal and low-pressure forms. In particular, it proposes that this phenomenon can be explained by the combined effect of: (*a*) a reversal of interstitial fluid flow in the parenchyma, and (*b*) a reduction in the elastic modulus of the cerebral mantle.

Method. To investigate this hypothesis, these changes have been incorporated into a finite element computer simulation of CH, in which brain tissue is idealized as a sponge-like material. The fluid pressure in the lateral ventricles and the subarachnoid space has been set to 10 mmHg, while the fluid pressure inside the parenchyma has been set to 7.5 mmHg. The elastic moduli of white and gray matter have been set to the reduced values of 1 and 5 kPa, respectively.

Findings. The simulation revealed a substantial ventricular distension (6.5 mm mean outward displacement), which was accompanied by the appearance of stress concentrations in the cerebral mantle.

Interpretation. These results support the notion that a relative reduction in intraparenchymal fluid pressure coupled with low tissue elasticity can produce both a significant ventricular enlargement and periventricular solid stress concentrations.

Keywords: Communicating hydrocephalus; biomechanics; ventricular enlargement.

Introduction

Hydrocephalus presents many paradoxes including the distribution of periventricular tissue damage, association of ventricular dilatation with high blood pressure, specific neuropsychological deficits and lack of correlation in many cases between the size of ventricles, clinical symptoms and the efficacy of a shunt [25]. While it is easy to understand that ventricular distension in non-communicating hydrocephalus (NCH) can be attributed to a transmantle pressure gradient subsequent to obstruction of the aqueduct of Sylvius, it remains an unresolved question why in communicating hydrocephalus (CH) the ventricles continue to dilate despite free communication between ventricles and the subarachnoid space and a normalization of ICP [13].

Several authors have proposed explanations for ventricular enlargement, including: alterations in the viscoelastic properties of brain parenchyma [23, 33], raised mean ICP and intracranial pulse pressure [8], normal tissue stresses [16] and the existence of transmantle pressure gradients [4, 38]. However, none of these studies have been able to convincingly integrate theoretical considerations, drawn usually from continuum mechanics, with experimental and clinical observations.

In this article we propose the hypothesis that the chronic ventricular distension that accompanies CH can be explained by the combined effect of: (*a*) a reversal of interstitial fluid flow into the parenchyma, and (*b*) a reduced tissue elasticity.

Methods

Biomechanics was introduced to the study of hydrocephalus by Hakim *et al.* [14, 15, 16]. In their pioneering work they proposed that brain parenchyma can be regarded as "an open cell sponge made of viscoelastic material". Nagashima *et al.* [22] formalized this concept in terms of the theory of poroelasticity [3], which studies the deformation of porous elastic materials. Since then, the view of brain tissue as a poroelastic material has been used in a number of studies [18, 24, 37]. The deformation mechanics of a poroelastic material is described by Biot's equations. As these equations have no general analytical solution, an approximate or numerical solution needs to be computed using finite element analysis [40]. The anatomical infor-

mation required to construct the FE mesh for our simulation was obtained from a T2-weighted, horizontally-orientated MR image of a brain from a normal volunteer.

Although the material properties of brain tissue are incompletely defined, experimental evidence suggests that the normal stiffness value of brain tissue is in the range 10 to 100 kPa [12]. In the hydrocephalic brain there is indirect evidence in the form of histological data from experimental models [28–30] and reduced PVI clinical data [6, 10, 36] which suggests that the brain tissue elasticity is reduced. In this study we have assumed isotropic material properties of 1 kPa and 5 kPa for the elastic moduli of white and gray matter, respectively. A Poisson's ratio of 0.30 and an hydraulic conductivity of 10^{-11} m^4 N^{-1} s^{-1} has also been assumed. The fluid pressure in the lateral ventricles and the subarachnoid space has been defined at 10 mmHg, within the normal range of ICP.

While it is generally agreed that there is fluid exchange between the CSF and brain via perivascular spaces, the magnitude and direction of flow remains controversial [26]. Intraventricular dye-injection experiments have demonstrated that the brain parenchyma acts as a CSF sink during hydrocephalus [20] while ventricle perfusion experiments suggest that there is a reversal of transependymal flow of interstitial fluid from CSF to brain [27]. More recently it has been established that perivascular spaces serve as conduits to transport cerebral interstitial fluid (ISF) to both blood and lymph [5]. In order to simulate this behavior, a reduced fluid pressure inside the parenchyma has been defined at 7.5 mmHg. Intra-vascular pressure at different points of the cerebrovascular bed will differ from adjacent interstitial fluid pressure as the result of the interposed compliance of the vascular wall [7]. Therefore in this study interstitial fluid pressure refers to the extracellular space fluid pressure and not to venous pressure.

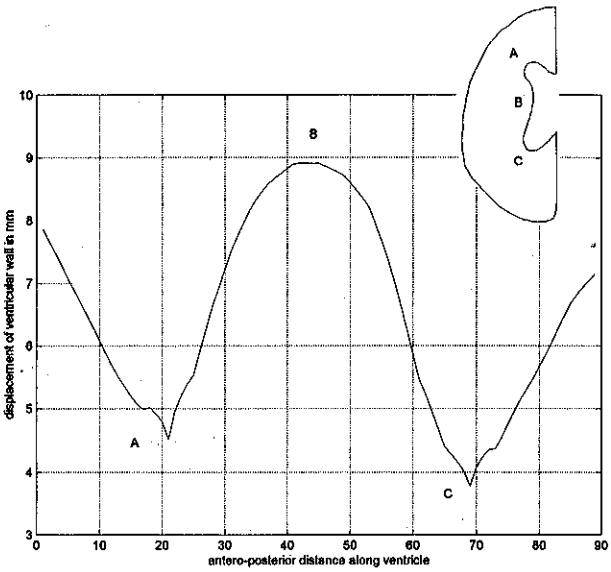

Fig. 1. This graph illustrates the magnitude of the outward displacement of the ventricular surface

Results

In accordance with clinical and experimental observations, the simulation of brain deformation during hydrocephalus, as defined by a sequence of FE meshes demonstrated progressive ventricular expansion. The magnitude of this enlargement at steady-state is illustrated in Fig. 1. The outward movement or displacement of the ventricular wall associated with this distension was heterogeneous along the antero–posterior direction of the ventricle. The maximum displacement occurred in the region of the thalamus with a value of almost 9 mm (Fig. 1, point B). This was followed by displacements of 8 and 9 mm in the anterior and posterior cyngulate gyri, respectively (Fig. 1, points A & C, respectively) and two regions of very small displacements near the anterior and posterior horns (4.5 and 5.0 mm, respectively). The overall mean outward displacement of the ventricles was 6.5 mm.

Discussion

Several studies have emphasized the importance of various physiological mechanisms in the development of chronic ventricular enlargement during CH [4, 8, 16]. Our FE simulation enabled us to investigate the effects of intraparenchymal fluid pressure and tissue elasticity on this process. Our theoretical analysis confirms that realistic alterations in these variables can result in both a significant ventricular enlargement and periventricular solid stress concentrations.

One of the early theories of normal pressure hydrocephalus (NPH) was that of Fishman [9] and Guinane [13] who proposed that it was not the absolute ventricular pressure, but rather the difference between ventricular pressure and the pressure over the cerebral convexity (the so-called transmantle pressure), that was the physiological determinant for ventricular dilatation. However, the existence of such a pressure gradient has been difficult to confirm. For example, Hoff and Barber [17] found an elevated transmantle pressure in three of four hydrocephalic patients and Conner [4] detected a gradient of 0.5 kPa (3.4 cm H_2O) in the cat. However, Shapiro *et al.* [32] failed to measure any pressure gradient. Regardless of these data, the measured values of Conner *et al.* are too small to create any substantial ventricular distention, given that they are is less than 5% of the typical range of the stiffness modulus of brain parenchyma. Hakim *et al.* [16] who also postulated the existence of a transmantle pressure gradient, proposed that one of the laws of mechanics could be applied to the understanding of hydrocephalus: $P = F/A$ where P, F, and A are

pressure, force and area, respectively. However, while this reference to Pascal's law enables the computation of changes in pressure, force and area on the *surface* on the brain, it provides no information about the deformation sustained *inside* the parenchyma. Finally, Pang and Altschuser [23] suggested that ventricular enlargement is related to an alteration of the viscoelastic modulus of the brain, secondary to expulsion of extracellular water from the brain parenchyma and to structural changes in brain tissues. However, changes in the mechanical properties of tissue without the presence of a pressure gradient cannot produce ventricular distension.

The theories discussed above provide insufficient explanations for ventricular distension. This is evident if we frame the discussion in terms of the fundamental principle established by Hooke in 1675 on the relationship between deformation and an applied force: $dL/L = (P/A)/E$, where dL is the change in length of the sample, L is the original length of the sample, P is the applied force, A is the cross-sectional area of the sample, and E is a proportionality constant known as Young's modulus [11]. Relative deformation or strain (i.e. dL/L) is directly proportional to an applied stress (i.e. P/A) and inversely proportional to the elasticity modulus (E) of the material. It follows that a substantial deformation of the cerebral mantle may be produced by the *combined* application of an increased pressure gradient together with a reduction in tissue elasticity. The application of this simple principle has

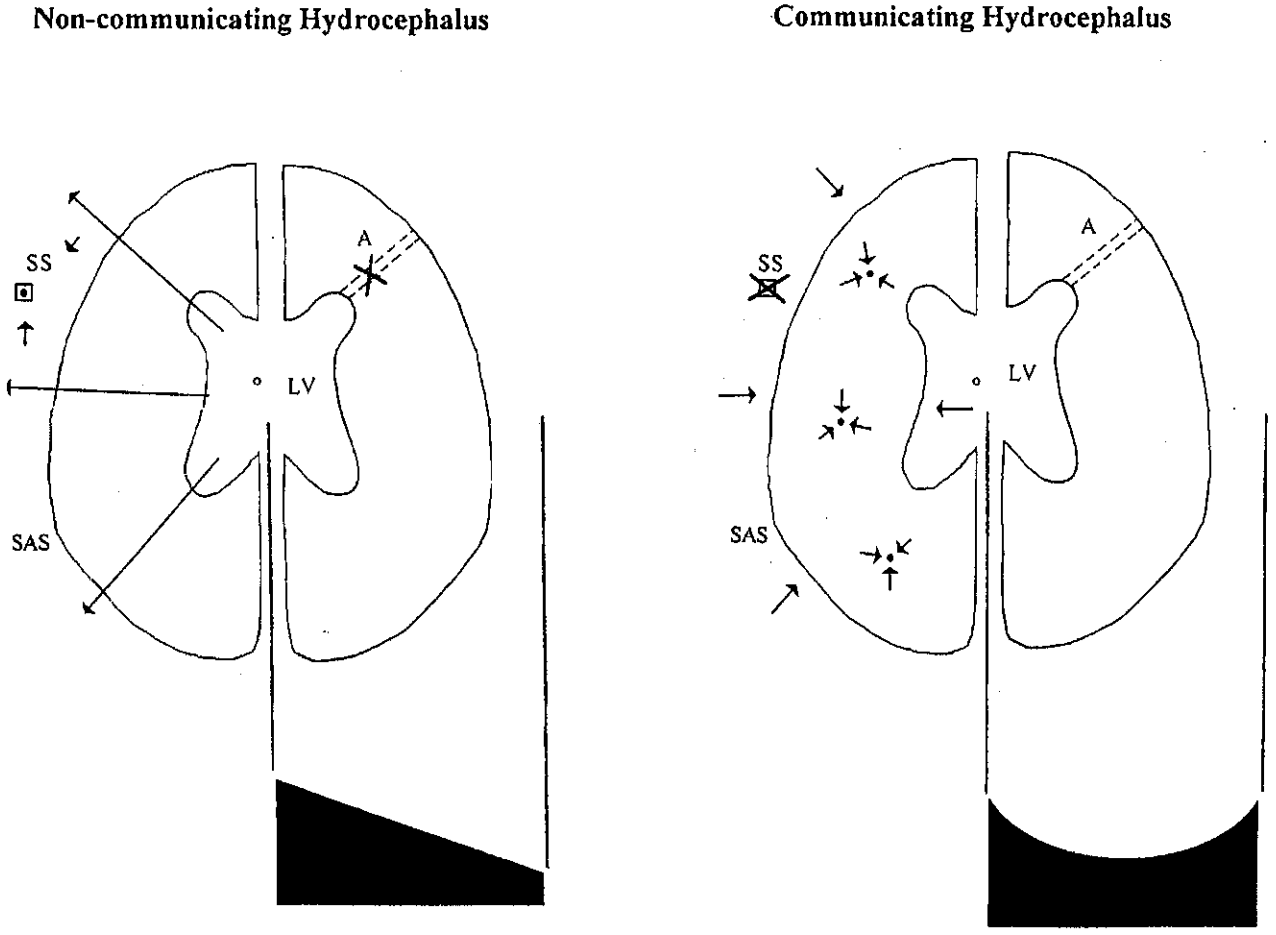

Fig. 2. This diagram illustrates the interaction of the various mechanisms involved in the development of non-communicating (*left*) and communicating (*right*) hydrocephalus. The arrows represent the interstitial CSF flow. The open dot represents sources of CSF. The closed dot represents sinks. The square represents the sagital sinus (*SS*). The cross represents an obstruction to CSF flow. The broken line represents the aqueduct of Sylvius. LV stands for lateral ventricles. SAS for subarachnoid space. In the case of NCH, due to the obstruction of of the aqueduct, a transmantle pressure (shown in black) is established between the LV and the SAS. CSF follows this gradient moving across the parenchyma to be finally absorbed at the SS. In the case of CH, there is no obstruction to the aqueduct but rather at the sagital sinus. An intramantle pressure gradient (shown in black) is produced, as the CSF is absorbed by the parenchyma. In both situations, ventricular distension occurs

led us to formulate the hypothesis that the chronic ventricular distension that accompanies CH can be explained by the combined effects of two factors: (a) a reversal of interstitial fluid flow in the parenchyma with a subsequent absorption of CSF by the tissue, and (b) a low tissue elasticity, brought about by a series of pathological changes.

Concerning the first factor, there is some convincing evidence for transependymal absorption of CSF. Early work on the pathways for CSF absorption postulated an alternative transventricular route [39] and these alternative pathways were demonstrated to be pressure dependent in the experimental hydrocephalic dog [2]. Subsequent studies substantiated the idea of transventricular absorption after demonstrating uptake of label into the parenchyma of various experimental models of hydrocephalus [1, 35].

Concerning the second factor, while the Young's modulus of bovine brain has been measured in vitro [12] no equivalent clinical or experimental in vivo hydrocephalic data exists. However many studies using the PVI as a measure of CSF compliance do provide some indirect evidence to support the notion that the stiffness modulus of tissue is reduced in CH. For example, the PVI was increased from the predicted normal value in a group of hydrocephalics at the time of shunt malfunction [10], in NPH patients [36], in low pressure hydrocephalus [23], infants [31] and in the experimental hydrocephalic cat when compared to controls [34]. The markedly increased PVI in these studies is presumably related to an alteration in the mechanical properties of the brain parenchyma, since the potential for deformation of the cranium is limited, especially in adults, given that cartilage is one hundred times stiffer than brain parenchyma [21]. Similarly, the vasculature represents only 7% of the total intracranial volume so that a substantial contribution to the changes in PVI is unlikely. Finally, the reduction in the stiffness modulus of the brain, from a physical point of view is also inferred from the major histopathological changes, such as neuronal injury, reactive astrocytosis and myelin degradation, in both experimental [19] and clinical hydrocephalus [30].

The crucial point in our theory is that the reversal of CSF transependymal flow implies that the fluid pressure is *smaller* in the parenchyma than in the surrounding CSF spaces. As a consequence of the movement of fluid into the tissue, a pressure gradient is established between the CSF spaces and the cerebral mantle: an *intramantle* pressure gradient.

Acknowledgments

AP is in receipt of a Wellcome Trust Training Fellowship in Mathematical Biology, and NGH of a Merck, Sharp & Dohme Research Fellowship.

References

1. Ahmadi J *et al* (1979) Evidence for transventricular absorption in the hydrocephalic dog. Invest Radiol 14: 432–437
2. Bering EA, Sato O (1963) Hydrocephalus: changes in the formation and absorption of cerebrospinal fluid within th ecerebral ventricles. J Neurosurg 20: 1050–1063
3. Biot MA (1941) General theory of three dimensional consolidation. J Appl Phys 12: 1244–1258
4. Conner ES, Foley L, Black PM (1984) Experimental normal-pressure hydrocephalus is accompanied by increased transmantle pressure. J Neurosurg 61: 322–327
5. Cserr HF, Harling-Berg CJ, Knopf PM (1992) Drainage of brain extracellular fluid into blood and deep cervical lymph and its immunological significance. Brain Pathol 2: 269–276
6. Czosnyka M *et al* (1993) Cerebrospinal compensation in hydrocephalic children. Childs Nerv Syst 9: 17–22
7. Czosnyka M *et al* (1993) CO2 cerebrovascular reactivity as a function of perfusion pressure – a modelling study. Acta Neurochir (Wien) 121: 159–165
8. Di Rocco C *et al* (1979) On the pathology of experimental hydrocephalus induced by artificial increase in endoventricular CSF pulse pressure. Childs Brain 5: 81–95
9. Fishman RA (1966) Occult hydrocephalus. N Engl J Med 274: 466–467
10. Fried A, Shapiro K (1986) Subtle deterioration in shunted childhood hydrocephalus. A biomechanical and clinical profile. J Neurosurg 65: 211–216
11. Fung YC (1994) A first course in continuum mechanics. Englewood Cliffs, New Jersey, Prentice Hall
12. Guillaume A *et al* (1997) Effects of perfusion on the mechanical behavior of the brain-exposed to hypergravity. J Biomech 30: 383–389
13. Guinane JE (1977) Why does hydrocephalus progress? J Neurol Sci 32: 1–8
14. Hakim CA, Hakim R, Hakim S (2001) Normal-pressure hydrocephalus. Neurosurg Clin N Am 12: 761–773, ix
15. Hakim S (1971) Biomechanics of hydrocephalus. Acta Neurol Latinoam [Suppl] 1: 169–194
16. Hakim S, Venegas JG, Burton JD (1976) The physics of the cranial cavity, hydrocephalus and normal pressure hydrocephalus: mechanical interpretation and mathematical model. Surg Neurol 5: 187–210
17. Hoff J, Barber R (1974) Transcerebral mantle pressure in normal pressure hydrocephalus. Arch Neurol 31: 101–105
18. Kaczmarek M, Subramaniam RP, Neff SR (1997) The hydromechanics of hydrocephalus: steady-state solutions for cylindrical geometry. Bull Math Biol 59: 295–323
19. Levine MS *et al* (1986) Quantitative morphology of medium-sized caudate spiny neurons in aged cats. Neurobiol Aging 7: 277–286
20. Miyagami M, Nakamura S, Moriyasu N (1975) [Hydrodynamic of the CSE under experimental occlusion of superior sagittal sinus (author's transl)]. No Shinkei Geka 3: 739–745
21. Mow VC *et al* (1980) Biphasic creep and stress relaxation of articular cartilage in compression? Theory and experiments. J Biomech Eng 102: 73–84

22. Nagashima T *et al* (1987) Biomechanics of hydrocephalus: a new theoretical model. Neurosurgery 21: 898–904
23. Pang D, Altschuler E (1994) Low-pressure hydrocephalic state and viscoelastic alterations in the brain. Neurosurgery 35: 643–655; discussion 655–656
24. Pena A *et al* (1999) Effects of brain ventricular shape on periventricular biomechanics: a finite-element analysis. Neurosurgery 45: 107–116; discussion 116–118
25. Punt CJ (1992) Principles of CSF diversion and alternative treatments. Hydrocephalus. In: Schurr PH, Polkey CE (eds) Oxford University Press, p 139–160
26. Rennels ML *et al* (1985) Evidence for a 'paravascular' fluid circulation in the mammalian central nervous system, provided by the rapid distribution of tracer protein throughout the brain from the subarachnoid space. Brain Res 326: 47–63
27. Rosenberg GA, Saland L, Kyner WT (1983) Pathophysiology of periventricular tissue changes with raised CSF pressure in cats. J Neurosurg 59: 606–611
28. Rubin RC *et al* (1976) Hydrocephalus: III. reconstitution of the cerebral cortical mantle following ventricular shunting. Surg Neurol 5: 179–183
29. Rubin RC *et al* (1976) Hydrocephalus: II. cell number and size, and myelin content of the pre-shunted cerebral cortical mantle. Surg Neurol 5: 115–118
30. Rubin RC *et al* (1976) Hydrocephalus: I. histological and ultrastructural changes in the pre-shunted cortical mantle. Surg Neurol 5: 109–114
31. Shapiro K, Fried A, Marmarou A (1985) Biomechanical and hydrodynamic characterization of the hydrocephalic infant. J Neurosurg 63: 69–75
32. Shapiro K *et al* (1987) Progressive ventricular enlargement in cats in the absence of transmantle pressure gradients. J Neurosurg 67: 88–92
33. Shapiro K, Marmarou A, Shulman K (1982) Abnormal brain biomechanics in the hydrocephalic child. From: concepts in pediatric neurosurgery vol 2. Pediatr Neurosurg 19: 216–222; discussion 223
34. Shapiro K *et al* (1985) Experimental feline hydrocephalus. The role of biomechanical changes in ventricular enlargement in cats. J Neurosurg 63: 82–87
35. Strecker EP *et al* (1973) Cerebrospinal fluid absorption in communicating hydrocephalus. Evaluation of transfer of radioactive albumin from subarachnoid space to plasma. Neurology 23: 854–864
36. Tans JT, Poortvliet DC (1988) Reduction of ventricular size after shunting for normal pressure hydrocephalus related to CSF dynamics before shunting. J Neurol Neurosurg Psychiatry 51: 521–525
37. Tenti G, Drake JM, Sivaloganathan S (2000) Brain biomechanics: mathematical modeling of hydrocephalus. Neurol Res 22: 19–24
38. White DN *et al* (1979) The limitation of pulsatile flow through the acqueduct of Sylvius as a cause of hydrocephalus. J Neurol Sci 42: 11–51
39. Wislocki GB, Putnam TJ (1921) Absorption from the ventricles in experimentally produced internal hydrocephalus. Am J Anatomy 29: 313–316
40. Zienkiewicz OC, Taylor RL (1991) The finite element method. McGraw-Hill

Correspondence: M. Czosnyka, Department of Neurosurgery, Box 167 Addenbrooke's Hospital, Cambridge CB2 2QQ, UK.

Printed in Austria